bioRxiv preprint doi: https://doi.org/10.1101/2020.04.02.022335; this version posted April 3, 2020. The copyright holder for this preprint (which was not certified by peer review) is the author/funder, who has granted bioRxiv a license to display the preprint in perpetuity. It is made available under aCC-BY-NC 4.0 International license.

Rapid stimulus-driven modulation of slow ocular position drifts

Tatiana Malevich[1, 2, 3]**, Antimo Buonocore[1, 2]**, Ziad M. Hafed[1, 2]*

[1] Werner Reichardt Centre for Integrative Neuroscience, Tuebingen University, Tuebingen, Germany
[2] Hertie Institute for Clinical Brain Research, Tuebingen University, Tuebingen, Germany
[3] Graduate School of Neural and Behavioural Sciences, International Max-Planck Research School, Tuebingen University, Tuebingen, Germany

* Correspondence to: ziad.m.hafed@cin.uni-tuebingen.de

** Contributed equally

Corresponding author information:

Ziad M. Hafed
Werner Reichardt Centre for Integrative Neuroscience
Tübingen University
Otfried-Müller Str. 25
Tübingen, Germany
72076
ziad.m.hafed@cin.uni-tuebingen.de

bioRxiv preprint doi: https://doi.org/10.1101/2020.04.02.022335; this version posted April 3, 2020. The copyright holder for this preprint (which was not certified by peer review) is the author/funder, who has granted bioRxiv a license to display the preprint in perpetuity. It is made available under aCC-BY-NC 4.0 International license.

Summary

Eye position changes subtly even when perfect gaze fixation is attempted [1-5]. Such "fixational" eye movement comes in two primary flavors: microsaccades, which resemble large saccades [6-8] and rapidly shift gaze position by a minute amount; and ocular position drifts, which are even smaller and slower movements [1, 2, 4, 5, 9-13]. The mechanisms for generating and influencing microsaccades have received much attention [6, 14, 15]. Despite contrary ideas in the past century, a now accepted property of microsaccades is that, like larger saccades, they are not random but are very systematically [16-24] and rapidly [19-21, 25, 26] influenced by peripheral as well as foveal visual stimuli, among other factors [14, 27]. In stark contrast, the brain mechanisms for controlling ocular position drifts are unknown; these movements continue to be thought of as random, often being modeled as random walk processes [28-32]. Here we used precise eye tracking in three well trained rhesus macaque monkeys to show that ocular position drifts can exhibit highly systematic stimulus-driven modulations in both speed and direction. These modulations have a very short latency, and they are stimulus-tuned, binocular, and independent of convergence responses or starting eye positions. Their amplitudes are sufficient to move images across individual cone photoreceptors in the fovea or multiple rod photoreceptors in some peripheral zones. Our results, coupled with evidence that drift statistics adapt to a variety of behavioral task constraints [13, 26, 33-35], strongly motivate deeper research into the neurophysiological mechanisms controlling incessant ocular position drifts in between saccades.

bioRxiv preprint doi: https://doi.org/10.1101/2020.04.02.022335; this version posted April 3, 2020. The copyright holder for this preprint (which was not certified by peer review) is the author/funder, who has granted bioRxiv a license to display the preprint in perpetuity. It is made available under aCC-BY-NC 4.0 International license.

Results

Short-latency, stimulus-driven ocular position drift response

We analyzed microsaccade-free fixation after a visual transient. In a first experiment, each monkey fixated a white spot over a gray background spanning approximately +/- 15 deg horizontally and +/- 11 deg vertically. At a random time, the display changed: one entire half (right or left) became black (split view stimulus); and a half-circle of 0.74-deg radius around the fixated position remained gray, in order to maintain view of the stable fixation spot (Methods). In trials without microsaccades (-100 to 200 ms from stimulus onset), a highly repeatable short-latency drift response occurred. This drift response is illustrated in Fig. 1A, B for monkey A, in which we tracked the left eye using the precise scleral search coil technique [36, 37]; the response measured in the two other monkeys, in which we measured right eye position, is shown in Fig. S1. Regardless of the tracked eye, and regardless of the steady-state stereotypical drift direction exhibited individually by a given monkey, there was always a robust upward position drift after stimulus onset. Importantly, it was clearly visible at the individual trial level (Figs. 1C, S1C, I). In one monkey (N), this upward drift response was sometimes initiated first by a much more short-lived and downward shift of eye position (of very small magnitude) before the flip to the upward drift (Fig. S1G-L).

We statistically assessed the onset and duration of the drift response in each monkey by computing 95% confidence intervals (Methods) around the average eye velocity traces. When the 95% confidence intervals between the stimulus and control velocity traces did not overlap for at least 20 consecutive milliseconds, we deemed the velocity response to be significant. In monkey A, the upward velocity pulse started at ~80 ms and lasted for ~60 ms (Fig. 1B). These values were ~60 ms and ~90 ms,

bioRxiv preprint doi: https://doi.org/10.1101/2020.04.02.022335; this version posted April 3, 2020. The copyright holder for this preprint (which was not certified by peer review) is the author/funder, who has granted bioRxiv a license to display the preprint in perpetuity. It is made available under aCC-BY-NC 4.0 International license.

respectively, for monkey M (Fig. S1B) and ~70 ms and ~100 ms, respectively, for monkey N (Fig. S1H). Note that Figs. 1A, S1A, G also show significance intervals for the eye position traces for completeness, although these provide a more conservative estimate of response onset time (Methods).

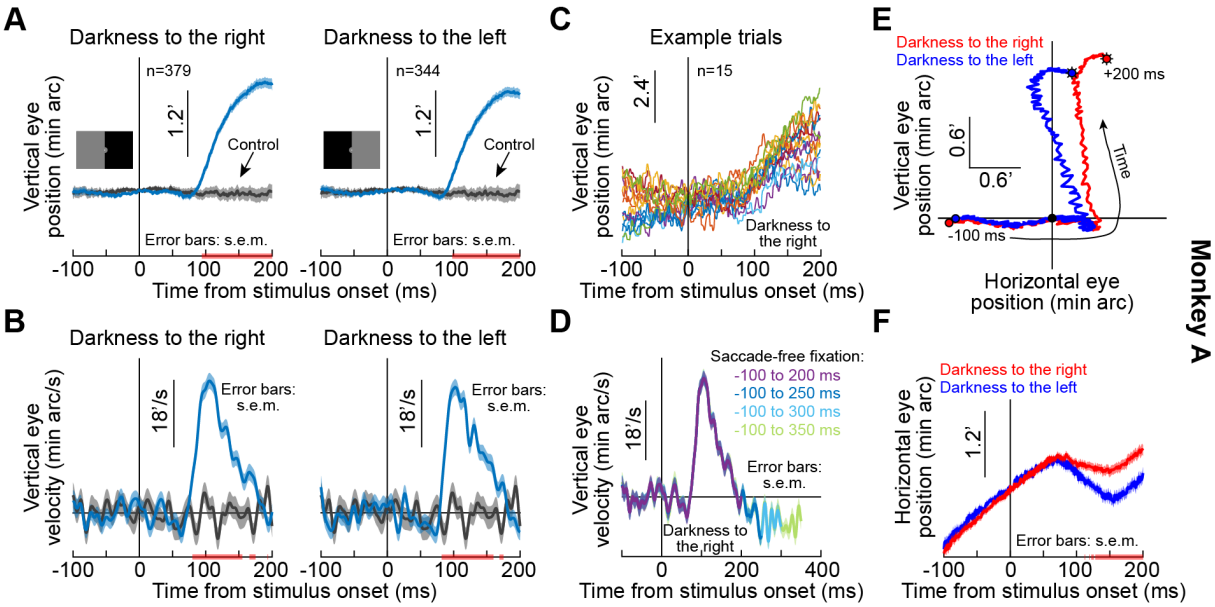

Figure 1 Short-latency, stimulus-driven ocular position drift response. (A) Vertical eye position (+/- s.e.m. bands) after split view stimulus onset. Compared to the no-stimulus condition (gray), the eye drifted upwards with short latency after stimulus onset. This happened for both right and left darkness stimuli (the two panels). We vertically aligned all starting eye positions at time 0 before averaging trials, to highlight the systematic change in eye position shortly after stimulus onset. **(B)** Same data as in **A** but for vertical eye velocity. A clear velocity pulse (much slower than that of microsaccades/saccades) is visible. **(C)** Individual trials demonstrating the drift response. The vertical position of each curve was jittered across the shown trials to facilitate visibility. **(D)** When we included progressively longer intervals of saccade-free fixation, we confirmed that the drift response (e.g. **B**) is transient. **(E, F)** Relative to starting eye position at stimulus onset, the drift response was predominantly vertical, but the horizontal component of eye position was also stimulus-dependent. Error bars in **F** denote s.e.m. The trajectories in **E** are two-dimensional plots of the average curves in **A**, **F**. All pink lines on x-axes indicate intervals in which the 95% confidence intervals of the two compared curves did not overlap. Also see Figs. S1, S2.

In all three monkeys, the drift response consisted of a predominantly upward velocity pulse reaching a peak speed of ~33-45 min arc/s, or ~0.55-0.75 deg/s (Figs. 1B, D, S1B, D, H, J) and a resultant displacement of ~2-3 min arc, or 0.034-0.05 deg (Figs. 1A, S1A, G). Such speeds and displacements are well within the detectability ranges

bioRxiv preprint doi: https://doi.org/10.1101/2020.04.02.022335; this version posted April 3, 2020. The copyright holder for this preprint (which was not certified by peer review) is the author/funder, who has granted bioRxiv a license to display the preprint in perpetuity. It is made available under aCC-BY-NC 4.0 International license.

of the visual system. For example, foveal cone photoreceptor separation in the rhesus macaque retina is ~1 min arc [38], and rod photoreceptor density can be even higher in the rod peak region [39]. Thus, the stimulus-driven drift response clearly modulates input images to the visual system.

The drift response was also transient: when we considered longer periods of saccade-free fixation, we did not notice increasing durations of drift response. Instead, the eye velocity "pulse" subsided, and eye position reverted back to its steady-state drift direction that was prominent, and stereotyped, in each monkey (Figs. 1D, S1D, J).

The drift response also showed horizontal direction dependence on the stimulus properties. In all three monkeys, the horizontal component of the eye movement during the drift pulse was systematically biased by the side of darkness (Figs. 1E, F, S1E, F, K, L): the upward drift tilted rightward when the darkness was on the right of gaze and leftward when it was on the left, and these results were statistically significant (pink intervals on all relevant x-axes of plots; Methods). The horizontal component of eye position therefore reacted to the spatial position of the luminance transient. This was our first evidence that the drift response can be stimulus-specific, a property that we revisit below.

The drift response is neither an eye tracking artifact nor a convergence reflex

We considered the possibility that the stimulus-driven drift response was part of a near reflex triad (convergence, accommodation, and pupil constriction) [40]. For example, the luminance transient may have been perceived by the monkey as a change in depth plane. However, this is unlikely to explain our observations: the

bioRxiv preprint doi: https://doi.org/10.1101/2020.04.02.022335; this version posted April 3, 2020. The copyright holder for this preprint (which was not certified by peer review) is the author/funder, who has granted bioRxiv a license to display the preprint in perpetuity. It is made available under aCC-BY-NC 4.0 International license.

horizontal bias as a function of stimulus appearance (e.g. Fig. 1E, F) occurred regardless of whether we tracked the right (monkeys M and N) or left (monkey A) eye. For example, if the drift was part of a convergence movement, it would not be biased rightward when tracked in the right eye (monkey M). We also explicitly tested for convergence in a later experiment, described below, in which we measured eye movements binocularly.

Our results also cannot be explained by variations in pupil diameter, which can cause artifactual eye drift measurements in video-based eye trackers [41-46]; in all of our analyses, we measured eye position using scleral search coils. Moreover, pupillary responses to stimulus transients exhibit significantly slower dynamics [47, 48]. To confirm this, we performed a control experiment in which we explicitly measured pupil diameter in one monkey (A) using a video-based eye tracker. Using a stimulus manipulation in which the upward drift response was clearly visible in the (left) eye (tracked with a scleral search coil), simultaneous measurement of pupil diameter in the other eye (tracked with a video-based eye tracker; Methods) revealed that the pupillary constriction caused by stimulus onset occurred later than the ocular position drift response (Fig. S2). It was futile to look for the drift response in the right eye, confirming that video-based eye trackers are not capable of resolving such small detail [41, 45, 46].

The drift response is a binocular eye movement

To directly investigate the convergence question, we next implanted one monkey (M) with a second scleral search coil, this time in the left eye. We could therefore measure binocular movements simultaneously. The monkey performed a new task in which we avoided a prolonged period of darkness in half of the display. Instead, the

bioRxiv preprint doi: https://doi.org/10.1101/2020.04.02.022335; this version posted April 3, 2020. The copyright holder for this preprint (which was not certified by peer review) is the author/funder, who has granted bioRxiv a license to display the preprint in perpetuity. It is made available under aCC-BY-NC 4.0 International license.

monkey steadily fixated with the original gray background. Then, for only one display frame (~8 ms), we flipped the luminance of the gray screen to black before it returned to gray again (Methods). We still observed a similar drift response (Fig. 2A, C). Importantly, the drift response occurred in both eyes simultaneously (Fig. 2A, C), and the horizontal component of eye position did not show an appreciable convergence response of similar magnitude (Fig. 2B, D). We confirmed this statistically; in a time interval capturing the drift response (50-140 ms), there was no statistically significant difference between right and left peak vertical or peak horizontal eye velocity (p=0.249, Z=1.15 for vertical and p=0.8321, Z=0.21 for horizontal; Wilcoxon rank sum test). Therefore, the stimulus-driven drift response (Figs. 1, S1, 2) is a binocular eye movement phenomenon that is independent of a convergence response.

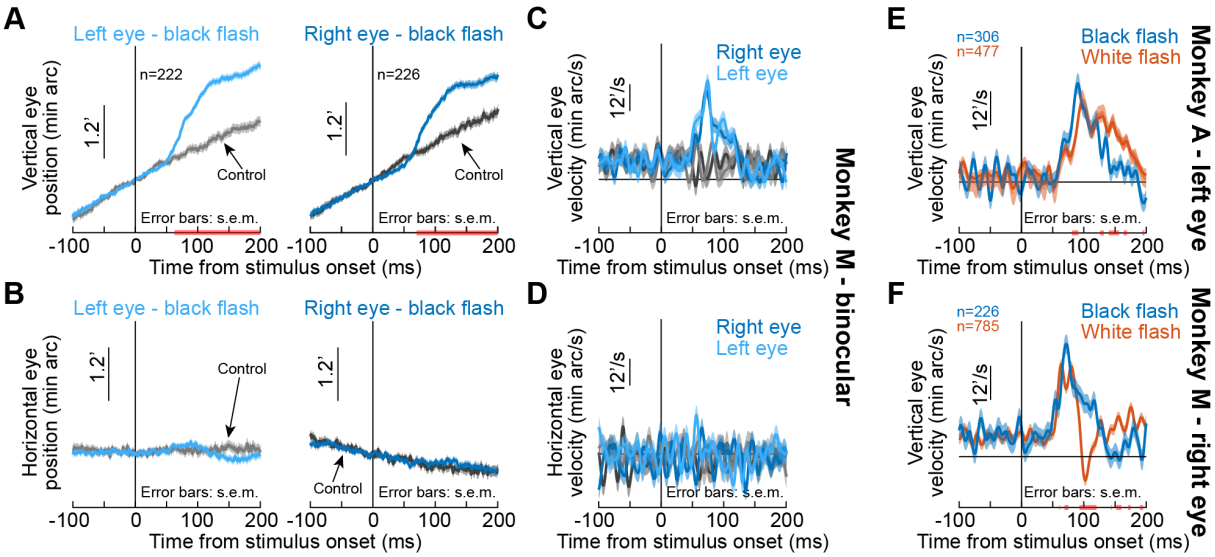

Figure 2 The drift response is a binocular eye movement. (A) Vertical eye position from monkey M during simultaneous measurements of the right and left eyes. The upward drift response (for a brief ~8 ms black flash covering the whole display) occurred binocularly. Note that this response superseded the monkey's stereotypical baseline slow upward drift, which was much slower (each monkey had a stereotypical baseline drift direction; Figs. 1, S1). **(B)** Horizontal eye position showed no evidence of convergence. **(C, D)** Same data with vertical and horizontal eye velocity, respectively. The drift response (**C**) was not associated with a convergence response (**D**). The lack of horizontal pink lines on the x-axes of **C**, **D** confirm that both eyes moved similarly. (**E**) In monkey A, we confirmed that the same paradigm (brief black flash) was still sufficient (bluish curve) to cause an upward drift response. When we switched the flash to white (reddish curve), the drift response still occurred. (**F**) Monkey M also showed a drift response for a white flash. Error bars in all panels denote s.e.m., and pink lines on the x-axes show periods in which the 95% confidence intervals of the two compared curves did not overlap. Also see Fig. S3.

bioRxiv preprint doi: https://doi.org/10.1101/2020.04.02.022335; this version posted April 3, 2020. The copyright holder for this preprint (which was not certified by peer review) is the author/funder, who has granted bioRxiv a license to display the preprint in perpetuity. It is made available under aCC-BY-NC 4.0 International license.

Naturally, we also tested a second monkey (A) on this new black fixation flash paradigm (albeit monocularly), and we still observed the drift response (Fig. 2E, bluish curve). Therefore, the drift response is not a peculiarity of the split view stimulus, and it still occurred in two monkeys under a completely different protocol.

The drift response is not the same as a steady-state up-shift in gaze in darkness

We next asked whether our observations were related to a previously reported steady-state upward eye position deviation in darkness [49-51]. After all, our split view stimulus introduced substantial darkness (in an already dark laboratory), and the fixation flash paradigm (Fig. 2A-D) also introduced darkness, although for just a fleeting moment. To test this, we ran the same two monkeys (A and M) on a third condition in which the entire display went from gray to white instead of black (again, for only ~8 ms; Methods). For both white and black flashes, a similar stimulus-driven transient ocular position drift response occurred (Fig. 2E, F). Statistically, peak eye velocity was significantly higher with black than white flashes in both monkeys ($p=4.2\times10^{-14}$, $Z=7.55$ for monkey A and $p=4.3\times10^{-5}$, $Z=4.09$ for monkey M; Wilcoxon rank sum test).

The drift response is feature-tuned

A significant swath (i.e. low spatial frequency) of luminance transience seemed necessary for the drift response. We did not observe the short-latency response as strongly with small localized targets briefly flashed to the right or left of fixation (Fig. S3). Our earlier experiments [26] also only revealed a later position modulation than the drift response being characterized in the current study.

bioRxiv preprint doi: https://doi.org/10.1101/2020.04.02.022335; this version posted April 3, 2020. The copyright holder for this preprint (which was not certified by peer review) is the author/funder, who has granted bioRxiv a license to display the preprint in perpetuity. It is made available under aCC-BY-NC 4.0 International license.

Given that visual responses in oculomotor areas like the superior colliculus (SC) preferentially represent low spatial frequencies [52], we therefore wondered whether the ocular position drift response could exhibit tuning to spatial frequency. We replicated the same full-screen flash paradigm in one monkey (M) but now with different spatial frequencies (0.55-6.8 cycles/deg; cpd). We saw clear preference for low spatial frequencies in the drift response, both in response latency and magnitude (Fig. 3A). To confirm this statistically, we searched for peak eye velocity in the interval 80-140 ms after stimulus onset (Fig. 3). We then characterized peak eye velocity and peak eye velocity latency as a function of spatial frequency using a Kruskal-Wallis test. There was an effect of spatial frequency on both peak velocity ($p=2.2\times10^{-16}$, $\chi^2(4)=79.49$) and peak velocity latency ($p=3.1\times10^{-17}$, $\chi^2(4)=83.56$). Post-hoc tests revealed that the drift response was earliest (adjusted $p<9.3\times10^{-8}$ against all other spatial frequencies) and strongest (adjusted $p<0.0021$ against the third to fifth spatial frequencies) for the lowest spatial frequency. With our split view stimulus and display geometry (tested in all three monkeys), the effective spatial frequency was even lower than 0.55 cpd, and the drift response appeared to be the strongest (Figs. 1, S1). Therefore, the ocular position drift response not only occurs early enough to reflect potential effects of early sensory responses in the oculomotor system (e.g. SC visual bursts; [52]), but it is also sensitive to stimulus specifics. In fact, when we ran yet another experiment with grating orientation, rather than spatial frequency, the drift response of the same monkey was again altered, and it displayed a form of orientation tuning (Fig. 3B; $p=0.01$, $\chi^2(4)=11.0$ for peak velocity and $p=0.0004$, $\chi^2(4)=18.5$ for peak velocity latency; Kruskal-Wallis test). Thus, ocular position drifts are sensitive, with short latency, to stimulus transients and their image features.

bioRxiv preprint doi: https://doi.org/10.1101/2020.04.02.022335; this version posted April 3, 2020. The copyright holder for this preprint (which was not certified by peer review) is the author/funder, who has granted bioRxiv a license to display the preprint in perpetuity. It is made available under aCC-BY-NC 4.0 International license.

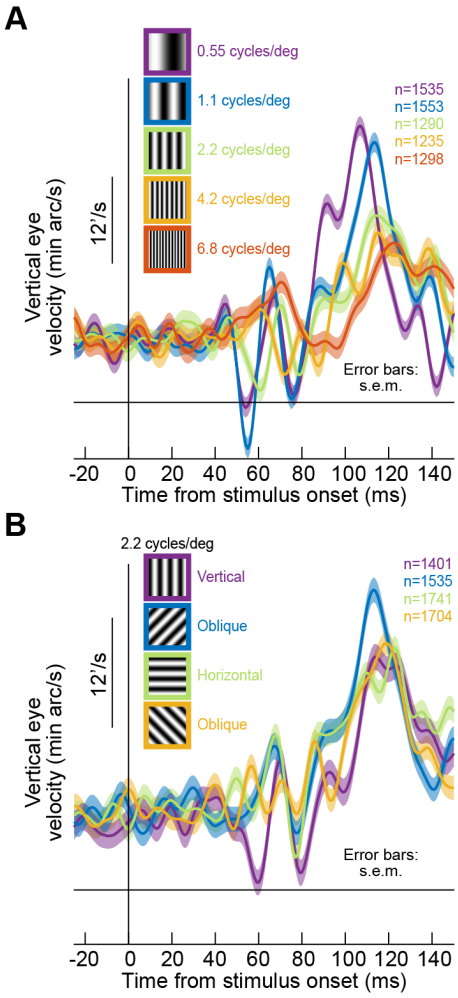

Figure 3 Stimulus tuning of the ocular position drift response. (A) We replaced the full-screen flash of Fig. 2 with a vertical grating of different spatial frequencies (Methods). The upward velocity pulse depended on spatial frequency; it occurred earlier, and had stronger amplitude, for low spatial frequencies. This is reminiscent of visual neural activity in the superior colliculus, an important oculomotor control circuit [52]. **(B)** Similarly, when we fixed spatial frequency and altered grating orientation, the drift response was also modulated. Ocular position drifts are therefore sensitive to stimulus manipulations. Error bars denote s.e.m.

The drift response happens at a time of complete saccade inhibition and is independent of starting eye position

In all of our analyses above, we isolated the properties of the drift response by analyzing saccade-free epochs. However, in reality, saccades could still occur even in our fixation paradigms. We therefore now considered the trials in which fixational

bioRxiv preprint doi: https://doi.org/10.1101/2020.04.02.022335; this version posted April 3, 2020. The copyright holder for this preprint (which was not certified by peer review) is the author/funder, who has granted bioRxiv a license to display the preprint in perpetuity. It is made available under aCC-BY-NC 4.0 International license.

microsaccades did occur. We found a remarkably complementary nature between the timing of microsaccades and the timing of the ocular position drift response. Specifically, it was long known that microsaccade likelihood decreases dramatically shortly after visual transients [18, 20, 25, 53-55]. We replicated this finding in all of our three monkeys, and we also compared the timing of the drift response to the timing of such saccadic inhibition (Fig. 4A-F; split view stimulus). The drift response occurred when it was least likely to observe microsaccades. Moreover, the drift response could still occur with nearby microsaccades before or after it (Fig. 4G-I). This also happened in our other tasks (e.g. Fig. S4). Even though the mechanisms of (micro)saccadic inhibition are still debated, we recently hypothesized that sensory transients in the oculomotor system (e.g. SC) play a particularly important role [25]. The stimulus dependence of the ocular drift response (e.g. Fig. 3) and its timing relative to saccadic inhibition (and indeed relative to the timing of early sensory responses in the oculomotor system [52]) suggest that the ocular drift response is mechanistically linked to the circuits mediating saccadic inhibition; and particularly to the short-latency visual responses in these circuits. Future neurophysiological experiments will have to directly test this hypothesis.

bioRxiv preprint doi: https://doi.org/10.1101/2020.04.02.022335; this version posted April 3, 2020. The copyright holder for this preprint (which was not certified by peer review) is the author/funder, who has granted bioRxiv a license to display the preprint in perpetuity. It is made available under aCC-BY-NC 4.0 International license.

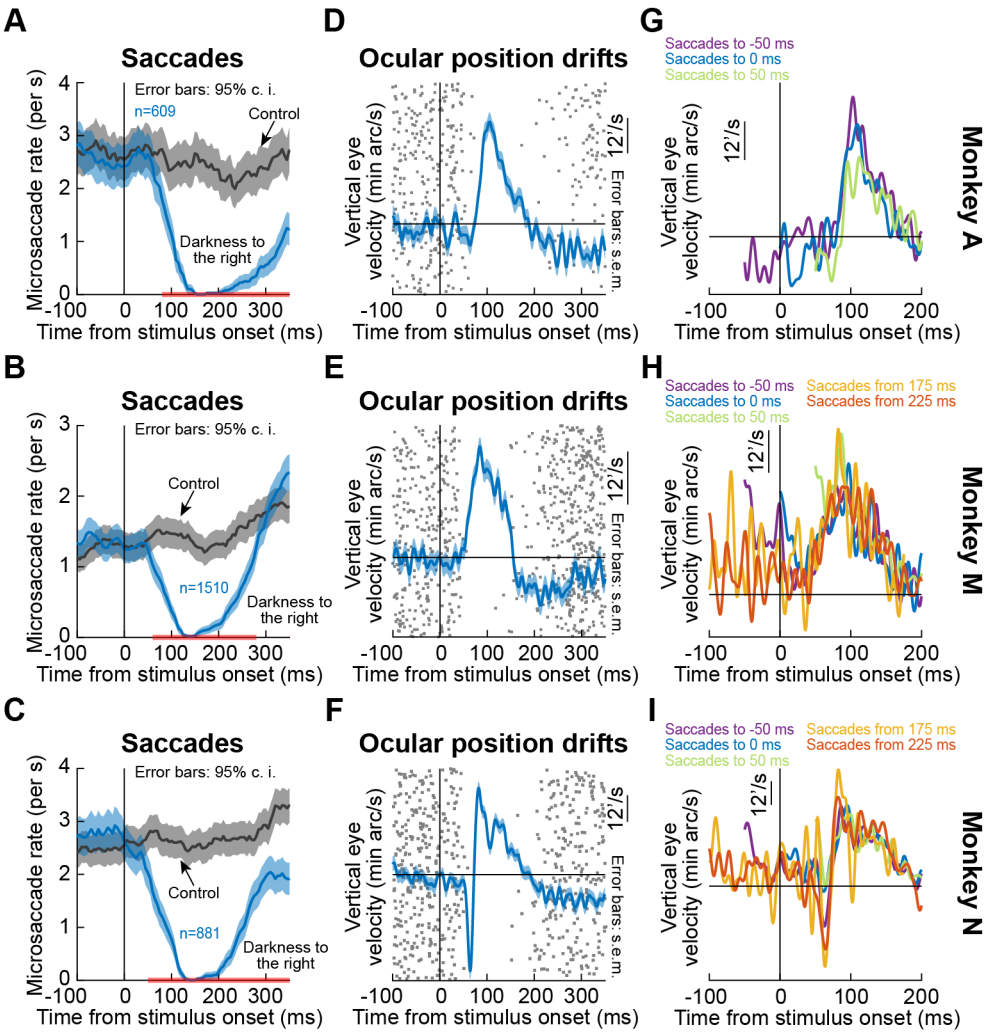

Figure 4 The drift response starts when saccades are inhibited. (A-C) Our monkeys exhibited known saccadic inhibition [18, 20, 25, 53-55] after stimulus onset (split view condition shown; Fig. S4 shows the fixation flash condition). Error bars denote 95% confidence intervals. **(D-F)** In the same sessions, saccade-free fixation epochs (no saccades from -100 to 350 ms) showed the ocular position drift response (error bars denote s.e.m.). The timing of this drift response was linked to the timing of saccadic inhibition (individual dots show individual trial rasters of microsaccade onset times from **A-C**). The drift response started when microsaccades were inhibited. **(G-I)** When we combined **A-C** and **D-F**, we found that even when microsaccades occurred near the time of drift response (i.e. before or after with shorter saccade-free epochs than in **D-F**), the drift response could still occur (in **G**, two curves are missing because they had <10 trials due to the prolonged saccadic inhibition profile in **A**). Error bars in **D-F** denote s.e.m. Also see Figs. S4-S6.

Finally, we checked whether the drift response could still occur with different starting eye positions. We divided trials based on eye position being above or below median vertical eye position across trials (Methods), and the same upward drift response was present (Fig. S5 shows these results from the black fixation flash paradigm in

bioRxiv preprint doi: https://doi.org/10.1101/2020.04.02.022335; this version posted April 3, 2020. The copyright holder for this preprint (which was not certified by peer review) is the author/funder, who has granted bioRxiv a license to display the preprint in perpetuity. It is made available under aCC-BY-NC 4.0 International license.

monkeys A and M). And, the drift response was too small to even elicit corrective downward microsaccades after it occurred: there was no clear bias for downward microsaccades after the drift response (Fig. S6).

Discussion

Our results demonstrate that slow fixational drift eye movements are systematically influenced by visual transients. These results motivate much deeper neurophysiological investigation of drift eye movement control, especially given that these eye movements are incessant and modulate the spatio-temporal statistics of input images to the visual system [32, 56, 57]. Classic brainstem neurophysiological studies of the oculomotor system (e.g. reviewed in [58]) are too coarse to provide the mechanistic insights necessary for explaining our observations. They need to be revisited with the perspective of understanding millisecond-by-millisecond tiny deviations of eye position during fixational drift.

Visual representations also need to be considered. Given the temporal transience of the drift response and its dependence on spatial frequency, it is likely that visual responses in oculomotor circuitry play a role. One possibility is that low spatial frequency stimuli increase the spatial uncertainty of intended gaze position. It is conceivable that such increased uncertainty, coupled with over representation of the upper visual field in the SC [59], as well as earlier visual bursts for upper visual field locations, results in transient upward drift responses. That is, increased spatial uncertainty increases the size of the active population of neurons, and if more neurons represent the upper visual field [59], then the transient response would be biased in the upward direction. Indeed, the SC influences eye position [60]; what remains is to understand whether instantaneous SC activity landscapes, in

bioRxiv preprint doi: https://doi.org/10.1101/2020.04.02.022335; this version posted April 3, 2020. The copyright holder for this preprint (which was not certified by peer review) is the author/funder, who has granted bioRxiv a license to display the preprint in perpetuity. It is made available under aCC-BY-NC 4.0 International license.

cooperation with the deeper brainstem, can explain instantaneous variations in fixational eye position. This would suggest fairly high level central nervous system control of these eye movements.

bioRxiv preprint doi: https://doi.org/10.1101/2020.04.02.022335; this version posted April 3, 2020. The copyright holder for this preprint (which was not certified by peer review) is the author/funder, who has granted bioRxiv a license to display the preprint in perpetuity. It is made available under aCC-BY-NC 4.0 International license.

Acknowledgements

We were funded by the Deutsche Forschungsgemeinschaft (DFG) through the Research Unit: FOR 1847 (project: HA6749/2-1). We were also funded by the Werner Reichardt Centre for Integrative Neuroscience (CIN; DFG EXC307) and the Hertie Institute for Clinical Brain Research. TM and ZMH were additionally supported by a CIN intramural grant (Mini_GK 2017-04).

Author Contributions

TM, AB, ZMH collected and analyzed the data. TM, AB, ZMH wrote and edited the manuscript.

Declaration of Interests

The authors declare no competing interests.

bioRxiv preprint doi: https://doi.org/10.1101/2020.04.02.022335; this version posted April 3, 2020. The copyright holder for this preprint (which was not certified by peer review) is the author/funder, who has granted bioRxiv a license to display the preprint in perpetuity. It is made available under aCC-BY-NC 4.0 International license.

References

1. Barlow, H.B. (1952). Eye movements during fixation. J Physiol *116*, 290-306.
2. Ratliff, F., and Riggs, L.A. (1950). Involuntary motions of the eye during monocular fixation. J Exp Psychol *40*, 687-701.
3. Steinman, R.M., Haddad, G.M., Skavenski, A.A., and Wyman, D. (1973). Miniature eye movement. Science *181*, 810-819.
4. Nachmias, J. (1959). Two-dimensional motion of the retinal image during monocular fixation. J Opt Soc Am *49*, 901-908.
5. Nachmias, J. (1961). Determiners of the drift of the eye during monocular fixation. J Opt Soc Am *51*, 761-766.
6. Hafed, Z.M. (2011). Mechanisms for generating and compensating for the smallest possible saccades. Eur J Neurosci *33*, 2101-2113.
7. Zuber, B.L., Stark, L., and Cook, G. (1965). Microsaccades and the velocity-amplitude relationship for saccadic eye movements. Science *150*, 1459-1460.
8. Rolfs, M. (2009). Microsaccades: small steps on a long way. Vision Res *49*, 2415-2441.
9. Poletti, M., and Rucci, M. (2015). A compact field guide to the study of microsaccades: Challenges and functions. Vision Res.
10. Ditchburn, R.W., and Ginsborg, B.L. (1953). Involuntary eye movements during fixation. J Physiol *119*, 1-17.
11. St Cyr, G.J., and Fender, D.H. (1969). The interplay of drifts and flicks in binocular fixation. Vision Res *9*, 245-265.
12. Martins, A.J., Kowler, E., and Palmer, C. (1985). Smooth pursuit of small-amplitude sinusoidal motion. J Opt Soc Am A *2*, 234-242.
13. Skinner, J., Buonocore, A., and Hafed, Z.M. (2019). Transfer function of the rhesus macaque oculomotor system for small-amplitude slow motion trajectories. J Neurophysiol *121*, 513-529.
14. Hafed, Z.M., Chen, C.-Y., and Tian, X. (2015). Vision, perception, and attention through the lens of microsaccades: mechanisms and implications. Frontiers in systems neuroscience *9*, 167.
15. Krauzlis, R.J., Goffart, L., and Hafed, Z.M. (2017). Neuronal control of fixation and fixational eye movements. Philos Trans R Soc Lond B Biol Sci *372*.
16. Hafed, Z.M., and Clark, J.J. (2002). Microsaccades as an overt measure of covert attention shifts. Vision Res *42*, 2533-2545.

bioRxiv preprint doi: https://doi.org/10.1101/2020.04.02.022335; this version posted April 3, 2020. The copyright holder for this preprint (which was not certified by peer review) is the author/funder, who has granted bioRxiv a license to display the preprint in perpetuity. It is made available under aCC-BY-NC 4.0 International license.

17. Engbert, R., and Kliegl, R. (2003). Microsaccades uncover the orientation of covert attention. Vision Res *43*, 1035-1045.

18. Hafed, Z.M., Lovejoy, L.P., and Krauzlis, R.J. (2011). Modulation of microsaccades in monkey during a covert visual attention task. Journal of Neuroscience *31*, 15219-15230.

19. Rolfs, M., Kliegl, R., and Engbert, R. (2008). Toward a model of microsaccade generation: the case of microsaccadic inhibition. J Vis *8*, 5 1-23.

20. Hafed, Z.M., and Ignashchenkova, A. (2013). On the dissociation between microsaccade rate and direction after peripheral cues: microsaccadic inhibition revisited. J Neurosci *33*, 16220-16235.

21. Tian, X., Yoshida, M., and Hafed, Z.M. (2016). A Microsaccadic Account of Attentional Capture and Inhibition of Return in Posner Cueing. Frontiers in systems neuroscience *10*, 23.

22. Thaler, L., Schutz, A.C., Goodale, M.A., and Gegenfurtner, K.R. (2013). What is the best fixation target? The effect of target shape on stability of fixational eye movements. Vision Res *76*, 31-42.

23. Ko, H.K., Poletti, M., and Rucci, M. (2010). Microsaccades precisely relocate gaze in a high visual acuity task. Nat Neurosci *13*, 1549-1553.

24. Engbert, R. (2006). Microsaccades: A microcosm for research on oculomotor control, attention, and visual perception. Prog Brain Res *154*, 177-192.

25. Buonocore, A., Chen, C.Y., Tian, X., Idrees, S., Munch, T.A., and Hafed, Z.M. (2017). Alteration of the microsaccadic velocity-amplitude main sequence relationship after visual transients: implications for models of saccade control. J Neurophysiol *117*, 1894-1910.

26. Tian, X., Yoshida, M., and Hafed, Z.M. (2018). Dynamics of fixational eye position and microsaccades during spatial cueing: the case of express microsaccades. J Neurophysiol *119*, 1962-1980.

27. Willeke, K.F., Tian, X., Buonocore, A., Bellet, J., Ramirez-Cardenas, A., and Hafed, Z.M. (2019). Memory-guided microsaccades. Nat Commun *10*, 3710.

28. Engbert, R., Mergenthaler, K., Sinn, P., and Pikovsky, A. (2011). An integrated model of fixational eye movements and microsaccades. P Natl Acad Sci USA *108*, E765-770.

29. Herrmann, C.J.J., Metzler, R., and Engbert, R. (2017). A self-avoiding walk with neural delays as a model of fixational eye movements. Scientific reports *7*, 12958.

30. Engbert, R., and Kliegl, R. (2004). Microsaccades keep the eyes' balance during fixation. Psychol Sci *15*, 431-436.

bioRxiv preprint doi: https://doi.org/10.1101/2020.04.02.022335; this version posted April 3, 2020. The copyright holder for this preprint (which was not certified by peer review) is the author/funder, who has granted bioRxiv a license to display the preprint in perpetuity. It is made available under aCC-BY-NC 4.0 International license.

31. Burak, Y., Rokni, U., Meister, M., and Sompolinsky, H. (2010). Bayesian model of dynamic image stabilization in the visual system. Proc Natl Acad Sci U S A *107*, 19525-19530.

32. Kuang, X., Poletti, M., Victor, J.D., and Rucci, M. (2012). Temporal encoding of spatial information during active visual fixation. Current biology : CB *22*, 510-514.

33. Chen, C.Y., and Hafed, Z.M. (2013). Postmicrosaccadic enhancement of slow eye movements. The Journal of neuroscience : the official journal of the Society for Neuroscience *33*, 5375-5386.

34. Intoy, J., and Rucci, M. (2020). Finely tuned eye movements enhance visual acuity. Nat Commun *11*, 795.

35. Cherici, C., Kuang, X., Poletti, M., and Rucci, M. (2012). Precision of sustained fixation in trained and untrained observers. Journal of vision *12*.

36. Judge, S.J., Richmond, B.J., and Chu, F.C. (1980). Implantation of magnetic search coils for measurement of eye position: an improved method. Vision Res *20*, 535-538.

37. Fuchs, A.F., and Robinson, D.A. (1966). A method for measuring horizontal and vertical eye movement chronically in the monkey. J Appl Physiol *21*, 1068-1070.

38. Rolls, E.T., and Cowey, A. (1970). Topography of the retina and striate cortex and its relationship to visual acuity in rhesus monkeys and squirrel monkeys. Exp Brain Res *10*, 298-310.

39. Wikler, K.C., Williams, R.W., and Rakic, P. (1990). Photoreceptor mosaic: number and distribution of rods and cones in the rhesus monkey retina. J Comp Neurol *297*, 499-508.

40. Myers, G.A., and Stark, L. (1990). Topology of the near response triad. Ophthalmic Physiol Opt *10*, 175-181.

41. Wyatt, H.J. (2010). The human pupil and the use of video-based eyetrackers. Vision research *50*, 1982-1988.

42. Drewes, J., Zhu, W., Hu, Y., and Hu, X. (2014). Smaller is better: drift in gaze measurements due to pupil dynamics. PLoS One *9*, e111197.

43. Hooge, I.T.C., Hessels, R.S., and Nystrom, M. (2019). Do pupil-based binocular video eye trackers reliably measure vergence? Vision Res *156*, 1-9.

44. Wildenmann, U., and Schaeffel, F. (2013). Variations of pupil centration and their effects on video eye tracking. Ophthalmic Physiol Opt *33*, 634-641.

45. Choe, K.W., Blake, R., and Lee, S.H. (2016). Pupil size dynamics during fixation impact the accuracy and precision of video-based gaze estimation. Vision Res *118*, 48-59.

bioRxiv preprint doi: https://doi.org/10.1101/2020.04.02.022335; this version posted April 3, 2020. The copyright holder for this preprint (which was not certified by peer review) is the author/funder, who has granted bioRxiv a license to display the preprint in perpetuity. It is made available under aCC-BY-NC 4.0 International license.

46. Kimmel, D.L., Mammo, D., and Newsome, W.T. (2012). Tracking the eye non-invasively: simultaneous comparison of the scleral search coil and optical tracking techniques in the macaque monkey. Front Behav Neurosci *6*, 49.

47. Pong, M., and Fuchs, A.F. (2000). Characteristics of the pupillary light reflex in the macaque monkey: metrics. J Neurophysiol *84*, 953-963.

48. Clarke, R.J., Zhang, H., and Gamlin, P.D. (2003). Characteristics of the pupillary light reflex in the alert rhesus monkey. J Neurophysiol *89*, 3179-3189.

49. Barash, S., Melikyan, A., Sivakov, A., and Tauber, M. (1998). Shift of visual fixation dependent on background illumination. J Neurophysiol *79*, 2766-2781.

50. Goffart, L., Quinet, J., Chavane, F., and Masson, G.S. (2006). Influence of background illumination on fixation and visually guided saccades in the rhesus monkey. Vision Res *46*, 149-162.

51. Snodderly, D.M. (1987). Effects of light and dark environments on macaque and human fixational eye movements. Vision Res *27*, 401-415.

52. Chen, C.Y., Sonnenberg, L., Weller, S., Witschel, T., and Hafed, Z.M. (2018). Spatial frequency sensitivity in macaque midbrain. Nat Commun *9*, 2852.

53. Reingold, E.M., and Stampe, D.M. (2002). Saccadic inhibition in voluntary and reflexive saccades. J Cogn Neurosci *14*, 371-388.

54. Buonocore, A., and McIntosh, R.D. (2008). Saccadic inhibition underlies the remote distractor effect. Exp Brain Res *191*, 117-122.

55. Edelman, J.A., and Xu, K.Z. (2009). Inhibition of voluntary saccadic eye movement commands by abrupt visual onsets. J Neurophysiol *101*, 1222-1234.

56. Rucci, M., and Victor, J.D. (2015). The unsteady eye: an information-processing stage, not a bug. Trends Neurosci.

57. Rucci, M., Iovin, R., Poletti, M., and Santini, F. (2007). Miniature eye movements enhance fine spatial detail. Nature *447*, 851-854.

58. Takahashi, M., and Shinoda, Y. (2018). Brain Stem Neural Circuits of Horizontal and Vertical Saccade Systems and their Frame of Reference. Neuroscience *392*, 281-328.

59. Hafed, Z.M., and Chen, C.Y. (2016). Sharper, Stronger, Faster Upper Visual Field Representation in Primate Superior Colliculus. Curr Biol *26*, 1647-1658.

60. Hafed, Z.M., Goffart, L., and Krauzlis, R.J. (2008). Superior colliculus inactivation causes stable offsets in eye position during tracking. J Neurosci *28*, 8124-8137.

61. Buonocore, A., Skinner, J., and Hafed, Z.M. (2019). Eye Position Error Influence over "Open-Loop" Smooth Pursuit Initiation. J Neurosci *39*, 2709-2721.

bioRxiv preprint doi: https://doi.org/10.1101/2020.04.02.022335; this version posted April 3, 2020. The copyright holder for this preprint (which was not certified by peer review) is the author/funder, who has granted bioRxiv a license to display the preprint in perpetuity. It is made available under aCC-BY-NC 4.0 International license.

62. Bellet, M.E., Bellet, J., Nienborg, H., Hafed, Z.M., and Berens, P. (2019). Human-level saccade detection performance using deep neural networks. J Neurophysiol *121*, 646-661.

63. Krauzlis, R.J., and Miles, F.A. (1996). Release of fixation for pursuit and saccades in humans: evidence for shared inputs acting on different neural substrates. J Neurophysiol *76*, 2822-2833.

bioRxiv preprint doi: https://doi.org/10.1101/2020.04.02.022335; this version posted April 3, 2020. The copyright holder for this preprint (which was not certified by peer review) is the author/funder, who has granted bioRxiv a license to display the preprint in perpetuity. It is made available under aCC-BY-NC 4.0 International license.

Methods

Ethics approvals

We tracked eye movements in 3 male rhesus macaque monkeys trained on behavioral eye movement tasks under head-stabilized conditions. The experiments were part of a larger neurophysiological investigation in the laboratory. All procedures and behavioral paradigms were approved by ethics committees at the Regierungspräsidium Tübingen, and they complied with European Union directives on animal research.

Animal preparation and laboratory setup

Monkey N was 12 years old at the time of the experiments; monkeys A and M were 6-9 years old. Each monkey was initially implanted with a titanium head holder under aseptic surgical conditions, as described earlier [33]. In a subsequent procedure, each monkey was additionally implanted with a scleral search coil in one eye (left for monkey A and right for monkeys N and M), in order to allow precise eye tracking using the magnetic induction technique [36, 37]. For some experiments in monkey M (e.g. Fig. 2), we also tracked eye movements binocularly. In this case, we performed an additional procedure to implant a search coil in this monkey's other eye. Eye coil implant procedures in our laboratory were described in detail earlier [33].

The laboratory setup consisted of a cathode ray tube (CRT) display placed in front of the monkey in an otherwise dim room. The display subtended approximately +/- 15 deg horizontally and +/- 11 deg vertically when the monkey fixated at its center, and it had a 120 Hz refresh rate. The monkey's head was surrounded by a cube generating electromagnetic fields for eye tracking (Remmel Labs). When we performed

bioRxiv preprint doi: https://doi.org/10.1101/2020.04.02.022335; this version posted April 3, 2020. The copyright holder for this preprint (which was not certified by peer review) is the author/funder, who has granted bioRxiv a license to display the preprint in perpetuity. It is made available under aCC-BY-NC 4.0 International license.

pupillometry (e.g. Fig. S2), we placed a video-based eye tracking camera (EyeLink 1000, desktop mount; SR-Research, Ontario, Canada) in front of the monkey under the CRT display. The eye tracking software output eye positions and pupil diameters (of the right eye) for synchronization with our existing real-time experiment control system, described in [21, 33].

All experiments involved initially fixating a white fixation spot over a gray background. The luminance of the gray background was 29.7 cd/m^2. The luminance of the white fixation spot was 86 cd/m^2. When we presented black stimuli, the luminance was < 0.02 cd/m^2. For all other stimuli (e.g. spatial frequencies), the details of the stimuli are provided below. Display resolution (~34-36 pixels/deg) was always higher than the Nyquist limit associated with the highest spatial frequency stimulus that we tested, and the display was linearized and calibrated before the experiments.

Behavioral tasks

Experiment 1 was called the split view stimulus paradigm. The monkey fixated a small white spot (approximately 5 x 5 min arc) presented over a gray background [33]. After an initial fixation interval (approximately 500-1400 ms), a stimulus onset occurred, which had the following properties. The stimulus onset was marked by turning one entire half of the display (right or left, randomly picked across trials) to black until the end of the trial (approximately 500-2000 ms after stimulus onset). The vertical edge associated with such a split view stimulus was gaze-contingently [21, 26, 33] updated, such that the edge between the light and dark regions of the retinal image was experimentally stabilized in real time relative to the fovea. This gaze-contingent image manipulation was relevant for other aspects of the task that are beyond the scope of the current analyses, especially because the current study

bioRxiv preprint doi: https://doi.org/10.1101/2020.04.02.022335; this version posted April 3, 2020. The copyright holder for this preprint (which was not certified by peer review) is the author/funder, who has granted bioRxiv a license to display the preprint in perpetuity. It is made available under aCC-BY-NC 4.0 International license.

focuses on time periods that are too short-lived to be affected by whether we used retinal image stabilization of the split view stimulus or not. To maintain visibility of the fixation spot despite the half-display of darkness that went right down its middle, we additionally enforced a kind of foveal sparing of the split view stimulus. Specifically, for a circle of radius 0.74 deg centered on instantaneous gaze position, we maintained background luminance even for the half of the circle that resided in the darkened half of the display (i.e. the circle was not split into a dark and bright half like the rest of the split view display). The fixation spot was always visible and always stable in the display (i.e. did not move gaze-contingently). We also interleaved control trials in this experiment that had identical timing; however, in this case, there was never a stimulus onset on the display (i.e. the monkey simply fixated steadily until trial end with no visual transients at all). We analyzed 5193, 2156, and 3860 trials in this experiment from monkeys M, A, and N, respectively. Typically, we collected 150-330 trials per session and repeated the experiment across multiple sessions.

Experiment 2 was called the black fixation flash experiment. Each monkey fixated a white spot over a gray background like in Experiment 1. After an initial fixation interval (approximately 550-1800 ms after initiating fixation), the entire display turned black for one single display frame (~8 ms duration given our 120 Hz refresh rate) before returning to its original state. Therefore, for one display frame, the fixation spot was rendered momentarily invisible. However, such a short duration of fixation spot occlusion is not expected to affect the eye movements that we analyzed (e.g. the drift response that we observed in this experiment was similar to that in Experiment 1 with a continuously visible fixation spot; see Results). In other control conditions in this experiment, we interleaved trials in which either no flash occurred at all, or in which

bioRxiv preprint doi: https://doi.org/10.1101/2020.04.02.022335; this version posted April 3, 2020. The copyright holder for this preprint (which was not certified by peer review) is the author/funder, who has granted bioRxiv a license to display the preprint in perpetuity. It is made available under aCC-BY-NC 4.0 International license.

the single frame flash was now a flash of a localized square of 1 x 1 deg dimensions centered at 2.1 deg horizontally either to the right or left of the fixation spot. The flashed square was also black, and the fixation spot was still visible in this case (because the flash did not occlude it). This experiment was similar to one we used recently under smooth pursuit conditions [61]. We analyzed 1671 and 1837 trials from monkeys M and A, respectively, in this experiment.

In our third experiment, we replicated Experiment 2 but with white rather than black flashes (the white fixation flash paradigm). We analyzed 5191 and 3112 trials from monkeys M and A, respectively, in this experiment.

Finally, Experiments 4 and 5 tested spatial frequency and orientation tuning, respectively, of the ocular position drift response in monkey M. We repeated the fixation flash paradigms described above. However, instead of full-screen black or white flashes, we presented a full-screen grating of a given stimulus property for approximately 260-700 ms. Across trials, we varied the spatial frequency (Experiment 4) or the orientation (Experiment 5) of the presented grating. There were no control or localized flash trials in these new experiments. Instead, we exploited the available numbers of trials to collect by varying the stimulus properties being tested across trials. For spatial frequency tuning, we tested 5 different spatial frequencies across trials (0.55, 1.1, 2.2, 4.2, and 6.8 cycles/deg; cpd). For orientation tuning, we tested 4 different orientations (vertical, 45 deg clockwise from vertical, horizontal, and 45 deg counterclockwise from vertical). Grating contrast was always maximal (100%). Also, across trials, we picked from two different grating phases (one in which the grating was white at the center of the display, near the fixation spot, and one in which the grating was black at the center of the display; i.e. a phase difference of π

bioRxiv preprint doi: https://doi.org/10.1101/2020.04.02.022335; this version posted April 3, 2020. The copyright holder for this preprint (which was not certified by peer review) is the author/funder, who has granted bioRxiv a license to display the preprint in perpetuity. It is made available under aCC-BY-NC 4.0 International license.

from the other condition). We analyzed 9967 trials from the spatial frequency manipulation and 9856 trials from the orientation manipulation.

To test for the relationship between the ocular position drift response and pupillary constrictions associated with stimulus onset, we measured pupil diameter in monkey A (Experiment 6). We ran the monkey on a variant of the fixation flash tasks that we knew would evoke a drift response (i.e. a full-screen flash of a visual pattern consisting of a high-contrast vertical grating). We confirmed such a drift response by measuring eye position using a scleral search coil. Simultaneously, we analyzed pupil diameter using a video-based eye tracker, and we analyzed variations in pupil diameter as a function of time from stimulus onset. This allowed us to relate the pupillary constriction response after stimulus onset to the ocular position drift response that we report in this study. Note that the video-based eye tracker was not suitable to detect the drift response in the same eye for which we measured the pupil. That is why we tracked the other eye with a scleral search coil. That is, we exploited our observation that the drift response is a binocular phenomenon (Fig. 2). We could have measured the pupil diameter in the coil eye, but our initial intent was to measure the drift response binocularly (with a coil in one eye and a video-based eye tracker for the other). However, it quickly became clear that the video-based eye tracker was simply not suitable for properly measuring the drift response, consistent with prior observations in the literature [41-43, 45, 46]. We analyzed 6203 trials from this comparison.

bioRxiv preprint doi: https://doi.org/10.1101/2020.04.02.022335; this version posted April 3, 2020. The copyright holder for this preprint (which was not certified by peer review) is the author/funder, who has granted bioRxiv a license to display the preprint in perpetuity. It is made available under aCC-BY-NC 4.0 International license.

Data analyses

We detected saccades and microsaccades using established methods in our laboratory [33, 62]. We also manually inspected all trials to ensure correct detection, and to also remove blinks.

To analyze our drift responses, we considered only trials in which there were no saccadic or blink events within an interval starting from -100 ms relative to stimulus onset and ending at +200 ms relative to stimulus onset. In additional control analyses, we extended this so-called saccade-free interval forward in time in steps of 50 ms until +350 ms after stimulus onset. That is, in the longest analysis interval that we considered, there were no saccadic or blink events between -100 ms and 350 ms from stimulus onset.

To absolutely ensure that we excluded any possibility of saccadic eye speeds (for even the smallest microsaccades) that might bias our measurements of average eye position across trials, we added one extra step after saccade detection, just as a sanity check: we inspected all accepted trials based on saccade detection and the above interval, and we ensured that eye velocity profiles did not have any clear outliers above the levels expected from ocular position drifts and measurement noise for a given session and monkey. This ensured that even rare electronic artifacts (lasting for only 1 ms or so) in scleral search coil measurements were not corrupting our ocular position drift interpretations.

We summarized the drift response properties by averaging eye position or velocity traces for a given stimulus type. When averaging eye positions, we aligned traces horizontally on stimulus onset time and vertically on the eye position that existed at

bioRxiv preprint doi: https://doi.org/10.1101/2020.04.02.022335; this version posted April 3, 2020. The copyright holder for this preprint (which was not certified by peer review) is the author/funder, who has granted bioRxiv a license to display the preprint in perpetuity. It is made available under aCC-BY-NC 4.0 International license.

this time. This way, we could observe the drift responses regardless of the absolute eye position that existed at trial onset. In other analyses (e.g. Fig. S5), we explicitly considered the effect of absolute eye position. Specifically, in each session, we estimated the trial-to-trial variance of eye position (due to fixational eye movements) at the time of stimulus onset (we averaged the final 50 ms of eye position data right before stimulus onset in each trial, and the across-trial distribution provided an estimate of fixation variability). Then, we considered only trials above the median vertical eye position across the population or only trials below the median vertical eye position. We then pooled the above-median and below-median populations across sessions to increase the numbers of observations (and, therefore, the statistical confidence of our results). For presentation in Fig. S5 of these median split data, we still aligned the eye positions at the time of stimulus onset as we did for the other figures (see above). This allowed us to directly demonstrate that the drift response was the same in timing and amplitude whether the starting eye position was below or above median eye position.

For analyzing microsaccades, we estimated microsaccade rate as a function of time from stimulus onset using similar methods to our earlier work [18, 25]. Briefly, we used a running window of width 80 ms, during which we estimated rate as the average number of movements observed per time window (and normalized to a unit of movements per second) [18]. We then stepped the window forward in time, in steps of 5 ms, starting from -300 ms and ending at +600 ms relative to stimulus onset.

We also checked whether the drift response happened when a nearby microsaccade still occurred (e.g. Fig. 4G-I). To do this, we binned trials based on the timing of

bioRxiv preprint doi: https://doi.org/10.1101/2020.04.02.022335; this version posted April 3, 2020. The copyright holder for this preprint (which was not certified by peer review) is the author/funder, who has granted bioRxiv a license to display the preprint in perpetuity. It is made available under aCC-BY-NC 4.0 International license.

microsaccades. For example, we looked for trials in which there was a microsaccade (or more) occurring up to a time of, say, +50 ms after stimulus onset. Then, we plotted saccade-free eye velocity after this time to look for the drift response. We used a similar procedure for other times earlier than +50 ms. For microsaccades after the drift response, we used a similar procedure. For example, we checked if there was a microsaccade (or more) starting from a time of, say, +225 ms after stimulus onset (i.e. after the ocular drift response). In this case, the drift response occurred earlier, so we plotted saccade-free eye velocity up to the time of, say, +225 ms.

To further relate microsaccades to the ocular drift response, we investigated whether the first microsaccade after the drift response was biased downwards in direction (e.g. to compensate for the predominantly upward drift response). We used the following procedure. In all of our saccade-free trials in the standard interval of -100 ms to +200 ms relative to stimulus onset, we searched for the first microsaccade to occur after this interval. We then plotted the angular distribution of this first microsaccade and related it to the control data without any stimulus onsets, but with the same analysis workflow of saccade-free fixation between -100 ms and +200 ms (Fig. S6).

For pupil diameter measurements, our data acquisition system output analog voltages proportional to pupil diameter values calculated by the video-based eye tracker. We stored digitized measurements of these voltages in synchrony with our stimulus events, and that is why we reported these measurements using arbitrary units in Fig. S2. We used the average pupil diameter in the final 100 ms before stimulus onset in a given trial as the baseline measurement. We subtracted this baseline measurement from all pupil measurements within the trial. Then, we

bioRxiv preprint doi: https://doi.org/10.1101/2020.04.02.022335; this version posted April 3, 2020. The copyright holder for this preprint (which was not certified by peer review) is the author/funder, who has granted bioRxiv a license to display the preprint in perpetuity. It is made available under aCC-BY-NC 4.0 International license.

averaged across trials. This allowed us to display the relative change in pupil diameter after stimulus onset (again, in arbitrary units). We ensured that we analyzed saccade-free epochs of pupil diameter, like we analyzed the ocular position drift responses in all other experiments. We measured saccades in both the video-based eye tracker signal as well as the other eye, which was tracked with a scleral search coil. This way, our analyses of pupil diameter dynamics after stimulus onset were comparable to the analyses of saccade-free ocular position drift responses that we report in this study. For the linear fits in Fig. S2, we used a piece-wise linear model to estimate the onset of the smooth ocular drift response or the onset of the pupil constriction. This approach is the same as that used for smooth pursuit eye movements earlier [63].

Finally, because we were dealing with very subtle eye position effects even in no-stimulus controls (e.g. Fig. 2A), we first confirmed that potential electronic drifts for our scleral search coil system cannot explain our results, and we did this before performing any of the analyses above. Specifically, sometimes, scleral search coil systems might exhibit a subtle drift in eye position calibration during the course of a given session (i.e. across tens of minutes or even hours). To confirm that such a potential technical artifact was too slow (if it existed at all) to account for even the baseline no-stimulus drift pattern of a given monkey in our data (e.g. Fig. 2A), we compared such baseline drift speed (which we deemed physiological) to any potential electronic drifts in eye tracker calibration across trials within a session. To do this, we measured average eye position in the final 30 ms before stimulus onset (including sham stimulus onset in control conditions). We then plotted this measurement as a function of trial number. Given the trial durations, this allowed us to estimate an “electronic drift speed” measure. When it existed, this electronic drift

bioRxiv preprint doi: https://doi.org/10.1101/2020.04.02.022335; this version posted April 3, 2020. The copyright holder for this preprint (which was not certified by peer review) is the author/funder, who has granted bioRxiv a license to display the preprint in perpetuity. It is made available under aCC-BY-NC 4.0 International license.

speed was at least an order of magnitude slower than baseline no-stimulus drift speeds of our monkeys. We are, therefore, confident that our results are physiological drifts of eye position, and not measurement artifacts.

Statistics

We used descriptive statistics throughout the study. All figures show and define error bars. We also did not show any average curves having fewer than 10 repetitions, because such few repetitions were deemed unreliable; this is the reason for the missing two curves in Fig. 4G in relation to the similar panels of Fig. 4H, I (saccades were simply too rare due to the saccadic inhibition shown in Fig. 4A). Typically, we had many more numbers of repetitions than 10, as shown in the insets of the figures.

To estimate temporal parameters such as the onset time of an ocular drift response, we compared measurements on trials with a stimulus onset to corresponding control trials without any stimulus onset. For each of the stimulus or control populations of repetitions, we estimated the 2x s.e.m. bounds (i.e. approximately 95% confidence intervals) surrounding the mean measurement. We then marked all time points in which such 95% confidence intervals of the two compared curves did not overlap. This was done using pink horizontal lines on all relevant x-axes in all figures. Due to noise (particularly in differentiated eye velocity measurements), there could be individual milliseconds or pairs of milliseconds in which there was no overlap between the 95% confidence intervals. We still displayed these time points in all figures. However, we consider a significant difference as one in which the 95% confidence intervals do not overlap for at least 20 consecutive milliseconds.

bioRxiv preprint doi: https://doi.org/10.1101/2020.04.02.022335; this version posted April 3, 2020. The copyright holder for this preprint (which was not certified by peer review) is the author/funder, who has granted bioRxiv a license to display the preprint in perpetuity. It is made available under aCC-BY-NC 4.0 International license.

We used the above procedures on either eye position or eye velocity independently, and we include results in all figures for both eye position and eye velocity curves. Because eye velocity computations necessarily involve some smoothing operation to regularize the noise associated with numerical differentiation, they introduce some temporal blurring of signals (both backwards and forwards in time). On the other hand, lack of overlap in the 95% confidence intervals of position traces would be too conservative, because it would estimate a later onset of the drift response (velocity is more sensitive than position for detecting onset of smooth eye movements). We therefore elected to show in the figures all statistical comparisons independently for both eye position and eye velocity traces, for the sake of completeness. In this regard, the position results can be considered to be conservative estimates of drift response onset time, whereas the velocity results can be considered to be slightly more liberal estimates. Numbers (e.g. p-values) reported in the text were based on eye velocity statistics, because eye velocity also allowed estimating the duration of the drift response (the end of which being when the eye velocity curve returned back to baseline with overlapping 95% confidence intervals).

In some cases, we additionally statistically compared drift responses across conditions (e.g. for right versus left eye). To do this, we defined a measurement interval based on the timing of the drift response that we observed (50-140 ms in black or white fixation flash paradigms and 80-140 ms in the spatial frequency and orientation paradigms). During this interval, we searched for peak eye velocity and characterized its magnitude and latency. When comparing two measurements (e.g. right versus left eye peak velocity latency), we used non-parametric Wilcoxon rank sum tests. When comparing multiple conditions (e.g. 5 different spatial frequencies),

bioRxiv preprint doi: https://doi.org/10.1101/2020.04.02.022335; this version posted April 3, 2020. The copyright holder for this preprint (which was not certified by peer review) is the author/funder, who has granted bioRxiv a license to display the preprint in perpetuity. It is made available under aCC-BY-NC 4.0 International license.

we used non-parametric Kruskal-Wallis tests. We used non-parametric tests because our measurements were not normally distributed.

bioRxiv preprint doi: https://doi.org/10.1101/2020.04.02.022335; this version posted April 3, 2020. The copyright holder for this preprint (which was not certified by peer review) is the author/funder, who has granted bioRxiv a license to display the preprint in perpetuity. It is made available under aCC-BY-NC 4.0 International license.

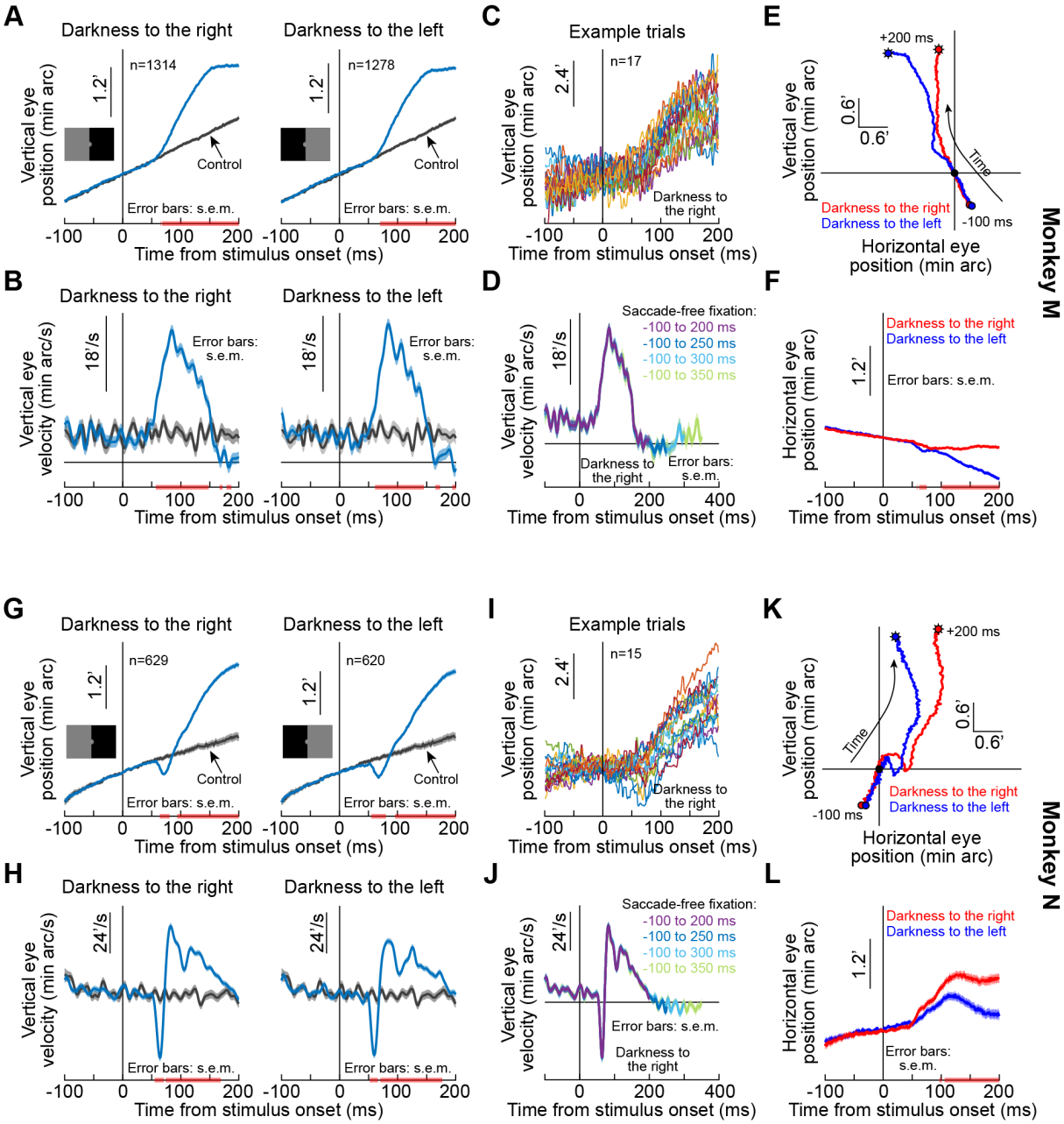

Figure S1, Related to Figure 1 Short-latency, stimulus-driven ocular position drift response in two additional monkeys besides the monkey shown in Fig. 1. This figure is formatted identically to Fig. 1. It shows very similar results from two additional monkeys, M and N. **(A-F)** Monkey M results. **(G-L)** Monkey N results. Error bars are defined in all relevant panels. The pink horizontal lines on various x-axes denote intervals in which the 95% confidence intervals around the two compared curves did not overlap.

bioRxiv preprint doi: https://doi.org/10.1101/2020.04.02.022335; this version posted April 3, 2020. The copyright holder for this preprint (which was not certified by peer review) is the author/funder, who has granted bioRxiv a license to display the preprint in perpetuity. It is made available under aCC-BY-NC 4.0 International license.

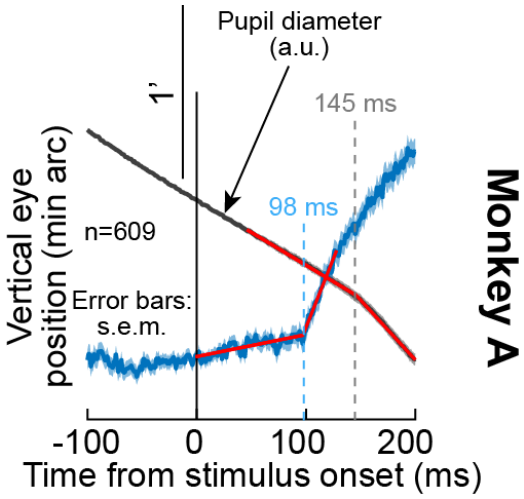

Figure S2, Related to Figure 1 The ocular position drift response occurred earlier than pupil diameter constriction occurring after stimulus onset. We measured pupil diameter in monkey A when a stimulus transient (high-contrast, full-screen vertical grating) was presented. The blue curve shows the ocular position drift response, replicating the results of Figs. 1, S1 in new experiments (scale bar is shown to the left of the 0-ms line). This response was measured with a scleral search coil in the left eye. The gray curve shows pupil diameter from the same set of trials, measured with a video-based eye tracker aimed at the right eye (the ocular position drift response was unresolvable in the right eye with the video-based eye tracker; Methods). To highlight the change in pupil diameter after stimulus onset within each trial, we averaged pupil diameter in the final 100 ms before stimulus onset, and we then subtracted this average from all pupil measurements within the trial. This aligned the pupil measurements across all trials in the y-axis dimension, isolating the relative changes in pupil diameter occurring after stimulus onset (Methods). This is a similar approach to our procedures for ocular position drift responses (e.g. Fig. 1 and the blue curve in the current figure). As can be seen, the inflection point of pupil diameter (indicated by the gray dashed vertical line at 145 ms), demonstrating stimulus-driven pupillary constriction, came significantly later than the onset of the ocular position drift response (indicated by the light blue dashed vertical line at 98 ms). Each inflection point was obtained by fitting a piece-wise linear model to each curve: a linear fit in an early interval before the onset of the ocular position drift response or pupil constriction, and a second linear fit in a later interval after the onset of the ocular position drift response or pupil constriction. This is similar to methods used earlier for estimating smooth pursuit onset latencies [S1]. The two linear fits per curve are shown in red. Error bars denote s.e.m. across trials.

bioRxiv preprint doi: https://doi.org/10.1101/2020.04.02.022335; this version posted April 3, 2020. The copyright holder for this preprint (which was not certified by peer review) is the author/funder, who has granted bioRxiv a license to display the preprint in perpetuity. It is made available under aCC-BY-NC 4.0 International license.

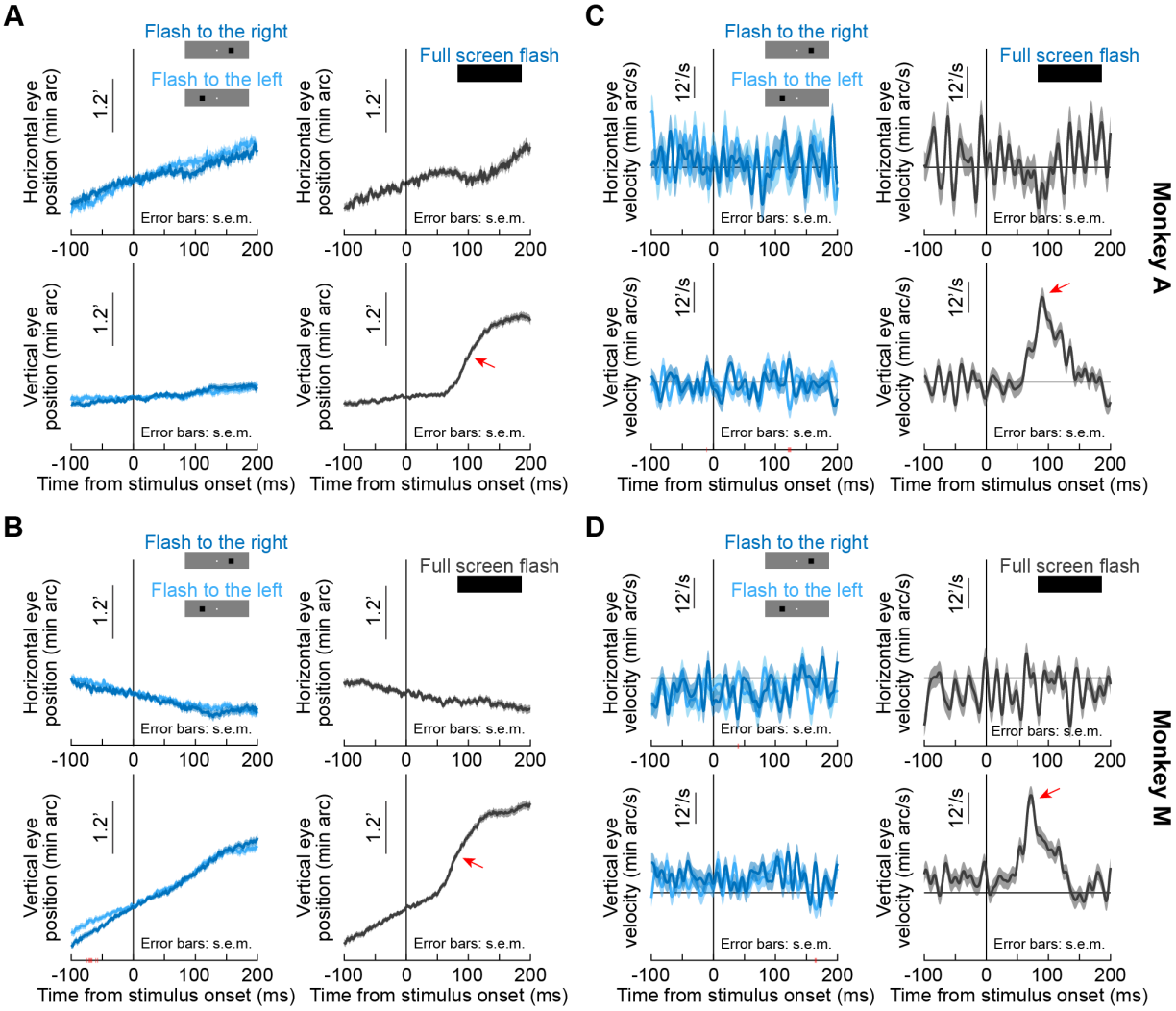

Figure S3, Related to Figure 2 Small localized stimulus onsets had minimal effects on ocular position drifts when compared to larger flashes. (A, B) Horizontal (top row in each panel) and vertical (bottom row in each panel) eye position in each of two monkeys (A and M) under different conditions. The left column in each panel shows data when small localized flashes were presented in the black fixation flash paradigm (Methods; similar results were obtained with the white fixation flash paradigm). The right column shows the full-screen flash results of Fig. 2 for comparison. All other conventions are like in Fig. 2. As can be seen, the upward drift response with full-screen flashes was much bigger than any responses to small localized stimuli. Consistent with this, there was no single contiguous interval longer than 8 ms in duration for which horizontal or vertical eye position differed between whether a localized flash was presented to the right or to the left of fixation (pink intervals on the x-axis of the bottom left panel of **B**, denoting when the 95% confidence intervals did not overlap with each other between the two compared curves). **(C, D)** Eye velocity measurements for the same data as in **A**, **B**. There were no time intervals during which the right and left flash eye velocity curves differed from each other (that is, there were no pink intervals on x-axes denoting a lack of overlap between 95% confidence intervals). We also confirmed that in the interval of 50-140 ms after stimulus onset, peak vertical eye velocity was not different between rightward and leftward localized flashes ($p=0.64$, $Z=0.47$ for monkey A and $p=0.92$, $Z=-0.10$ for monkey M; Wilcoxon rank sum test). A similar conclusion was also reached for peak horizontal eye velocity ($p=0.5$, $Z=-0.68$ for monkey A and $p=0.52$, $Z=-0.65$ for monkey M). Error bars in all panels denote s.e.m.

bioRxiv preprint doi: https://doi.org/10.1101/2020.04.02.022335; this version posted April 3, 2020. The copyright holder for this preprint (which was not certified by peer review) is the author/funder, who has granted bioRxiv a license to display the preprint in perpetuity. It is made available under aCC-BY-NC 4.0 International license.

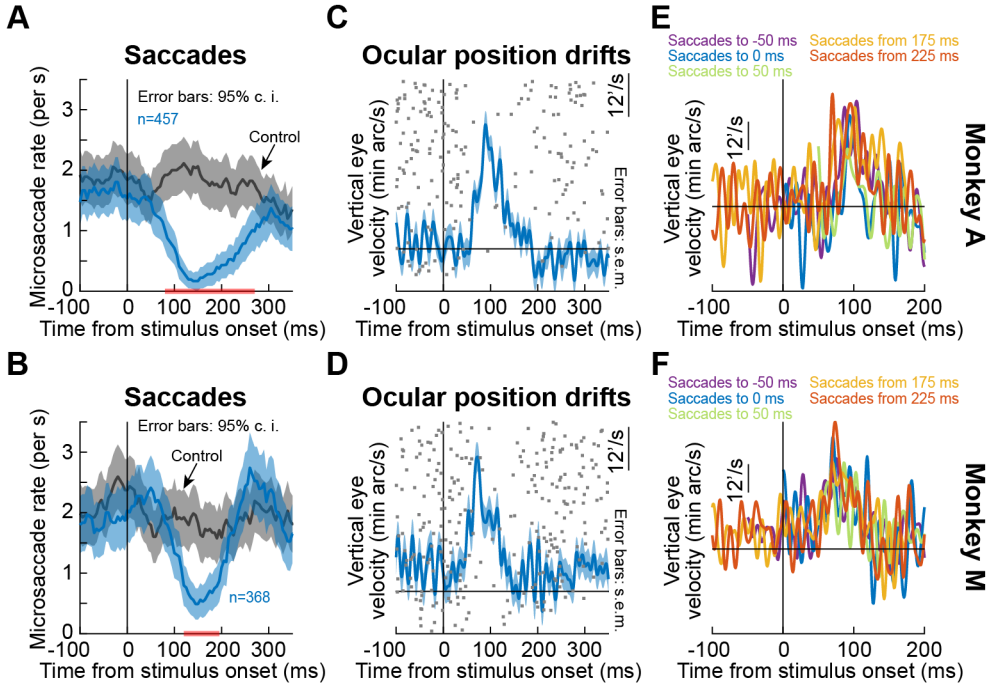

Figure S4, Related to Figure 4 The ocular position drift response occurred during saccadic inhibition, and it also occurred even with nearby saccades. This figure is formatted identically to Fig. 4. It shows similar results, but this time from the black fixation flash paradigm using full-screen flashes (the white fixation flash paradigm produced similar observations). **(A, B)** Microsaccade rate after full-screen flash onset in each monkey. The gray curve shows baseline microsaccade rate with no stimulus transient. **(C, D)** Ocular position drift response in each monkey during saccade-free fixation. To illustrate the timing of the drift response to saccadic inhibition, the dots indicate trial-by-trial rasters of microsaccade onset times during fixation. The drift response occurred when microsaccades were inhibited. **(E, F)** In each monkey, we inspected the ocular drift response when microsaccades still occurred near stimulus onset (different colors denote different microsaccade times as per the legends). The drift response still occurred, as in Fig. 4 with another paradigm and the inclusion of a third monkey. Error bars are defined in the respective panels (95% confidence intervals in **A**, **B**, and s.e.m. otherwise). All other conventions are similar to Fig. 4.

bioRxiv preprint doi: https://doi.org/10.1101/2020.04.02.022335; this version posted April 3, 2020. The copyright holder for this preprint (which was not certified by peer review) is the author/funder, who has granted bioRxiv a license to display the preprint in perpetuity. It is made available under aCC-BY-NC 4.0 International license.

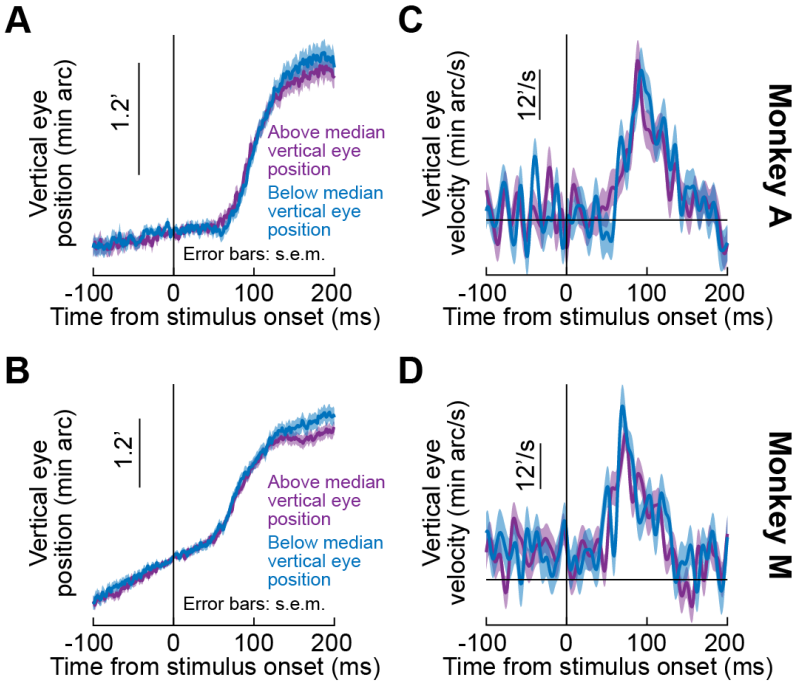

Figure S5, Related to Figures 1-4 Independence of the ocular position drift response from starting eye position. For each trial of the black fixation flash paradigm (full-screen flashes), we measured average eye position in the final 50 ms before stimulus onset. Across trials within a given session, this resulted in a population of starting eye positions. We split the trials within a session based on the median value of starting vertical eye position. We then measured the ocular position drift response for all sessions when only taking the "above" median group of the sessions (purple) and again when taking only the "below" median group of all sessions (bluish). **(A, B)** Position measurements in two monkeys. We vertically aligned traces (based on starting position at stimulus onset) in order to highlight the relative change in eye position associated with the ocular position drift response (similar to how we analyzed data in all other figures; e.g. Fig. 1). **(C, D)** Eye velocity measurements. In both eye position and eye velocity, the ocular drift response measurements were statistically very similar; there were no time intervals in which the 95% confidence intervals between the "above" and "below" median groups did not overlap with each other. We also confirmed that in the interval of 50-140 ms after stimulus onset, peak vertical eye velocity was not different between the two groups ($p=0.63$, $Z=0.48$ for monkey A and $p=0.46$, $Z=0.74$ for monkey M; Wilcoxon rank sum test). All other conventions are similar to our other analyses of the ocular position drift response (e.g. Fig. 1). Similar results were obtained with the split view stimulus and white fixation flash paradigms (e.g. $p=0.32$ [$Z=-1.01$], 0.62 [$Z=-0.5$] for monkeys A and M, respectively, in the white fixation flash paradigm, and $p>0.15$ [$Z=-1.46$, -0.82], $p>0.2$ [$Z=-0.55$, 1.27], and $p>0.85$ [$Z=0.01$, 0.19] for monkeys A, M, and N, respectively, in the split view stimulus paradigm; Z-values reported for right and left darkness for each monkey in the split view stimulus paradigm).

bioRxiv preprint doi: https://doi.org/10.1101/2020.04.02.022335; this version posted April 3, 2020. The copyright holder for this preprint (which was not certified by peer review) is the author/funder, who has granted bioRxiv a license to display the preprint in perpetuity. It is made available under aCC-BY-NC 4.0 International license.

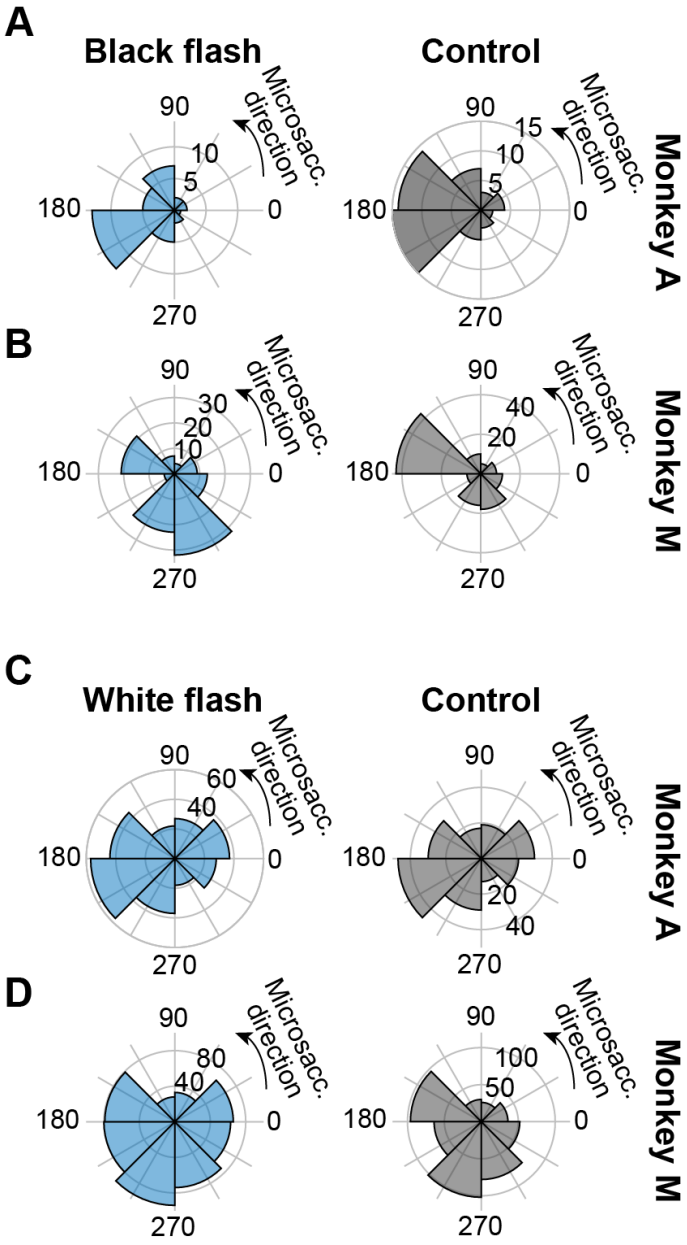

Figure S6, Related to Figure 4 The drift response was not systematically related to the direction of the first microsaccade to occur after it. We searched for the first microsaccade to occur after our standard designated saccade-free fixation interval of -100 ms to 200 ms relative to full-screen flash onset. Across trials, we then plotted the direction distribution of these first microsaccades. Each row shows the stimulus onset condition (left column) and the corresponding control condition without any full-screen stimulus flash (right column). **(A, B)** Black fixation flash paradigm. **(C, D)** White fixation flash paradigm. Similar results were obtained with the split view stimulus paradigm. In all cases, each monkey showed a stereotypical distribution of microsaccade directions in the control condition without any stimulus onset (e.g. predominantly leftward in the monkey A control data; right column). This distribution was largely unaltered after the upward ocular position drift response, despite some idiosyncratic variations in the ranges of microsaccade directions that occurred. This is expected: given how small the ocular position drift response is (e.g. Fig. 1), its amplitude is much smaller than the amplitude of microsaccades, and it is therefore unlikely to trigger a corrective downward microsaccade.

bioRxiv preprint doi: https://doi.org/10.1101/2020.04.02.022335; this version posted April 3, 2020. The copyright holder for this preprint (which was not certified by peer review) is the author/funder, who has granted bioRxiv a license to display the preprint in perpetuity. It is made available under aCC-BY-NC 4.0 International license.

References

S1. Krauzlis, R.J., and Miles, F.A. (1996). Release of fixation for pursuit and saccades in humans: evidence for shared inputs acting on different neural substrates. J Neurophysiol *76*, 2822-2833.